2022 IEEE-EMBS International Conference on Wearable and Implantable Body Sensor Networks (BSN)

Additively Manufactured Dry Electrodes for Biosignal Measurements

Gerrit Bücken
Fraunhofer IMTE, Fraunhofer Research Institution for Individualized and Cell-Based Medical Engineering
Lübeck, Germany
ORCID: 0000-0001-7534-6979

Thomas Friedrich
Fraunhofer IMTE, Fraunhofer Research Institution for Individualized and Cell-Based Medical Engineering
Lübeck, Germany
ORCID: 0000-0002-5907-4245

Roman Kusche
Fraunhofer IMTE, Fraunhofer Research Institution for Individualized and Cell-Based Medical Engineering
Lübeck, Germany
ORCID: 0000-0003-2925-7638

***Abstract*—The acquisition of electrophysiological signals, such as electrocardiography or electromyography, is an integral part of medical diagnostics and therapy. In the clinical environment, these signals are typically recorded using adhesive gel electrodes which have particularly good electrical characteristics. Outside this environment, however, these electrodes are not practical, since they have to be placed manually and can only be used once. Instead, the use of dry electrodes can be beneficial, especially in complex systems such as wearables or prostheses. Unfortunately, these electrodes are not widely commercially available and their electrical characteristics are hardly documented. One major challenge is the occurring high interface impedance between the electrode and the skin. In this study, dry electrodes with different contact surfaces made of conductive polylactide acid are designed, additively manufactured and the corresponding electrode-skin impedances are examined on human subjects. The influences of different electrode radii as well as surface structures on the electrode-skin interface impedance are compared with each other. The result of the investigation is that the impedance decreases as the contact area increases, which corresponds to the electrical equivalent circuit. However, the chosen structuring of the surface has a negative impact on the impedance, although the effective electrode surface was expected to be increased.**

***Index Terms*—Additive manufacturing, biosignals, dry electrodes, electrode-skin impedance, ECG, EMG, wearables**

I. Introduction

Since the human body is an ion conductor, but electronic measuring circuits are electron conductors, electrodes are required for the connection of several medical electrical measurement devices [1]. These electrochemical interfaces are complex and can significantly influence and even falsify the measurements. For many applications, such as electrocardiography (ECG), electromyography (EMG), electroencephalography (EEG) and bioimpedance analyses, low contact impedances are of particular importance [2]. These are often achieved by using adhesive gel electrodes with very stable electrical contact characteristics. However, these electrodes have to be placed manually to the correct positions and afterwards need to get electrically contacted. In addition, these electrodes are only commercially available in certain sizes and can only be used once. Another type of electrode, known from transcutaneous electrical nerve stimulation (TENS), are dry electrodes, typically made of carbonized polymers [3]. These can be used multiple times and can be permanently connected with cables. However, the resulting contact impedances are typically significantly higher than those of gel electrodes [4]. In addition, these electrodes are not available in various shapes and sizes. Therefore, the aims of this work are the design, the individual manufacturing of plastic electrodes and their investigation regarding the occuring contact impedance. To minimize these, the influences of electrode size and surface structures are investigated by means of subject measurements.

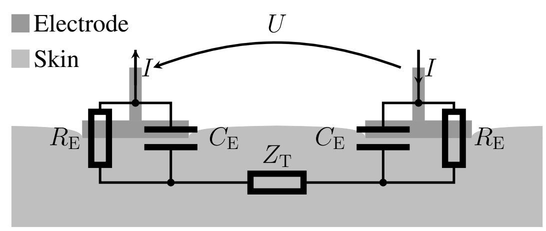

Fig. 1: Equivalent circuit diagram of the passive electrical behavior of electrode-skin contacts.

II. Materials and Methods

A. Electrode-Skin Equivalent Circuit

In order to describe and analyse the complex electrical behaviour of electrode-skin interfaces, a simplified electrical equivalent circuit, which is based on the models published in [1, 5], shown in Fig. 1, is used. Here, the occurring two electrode-skin impedances Z_{E} are assumed to be same and are represented by parallel connections of the ideal resistances R_{E} and capacitances C_{E}. The tissue impedance is represented by Z_{T}. The simplified assumption provides that the resistance of the electrical electrode-skin contact is inversely proportional to the contact area A_{E}. The capacitance, on the other hand, is proportional to the contact area. Since full contact between electrode and skin is assumed, the contact area is completely determined by the surface of the electrodes. This results in an inverse proportionality to the contact area for the parallel connection of resistance and capacitance, representing Z_{E}. Therefore, the magnitude of the resulting electrode-skin impedance decreases with increasing contact area.

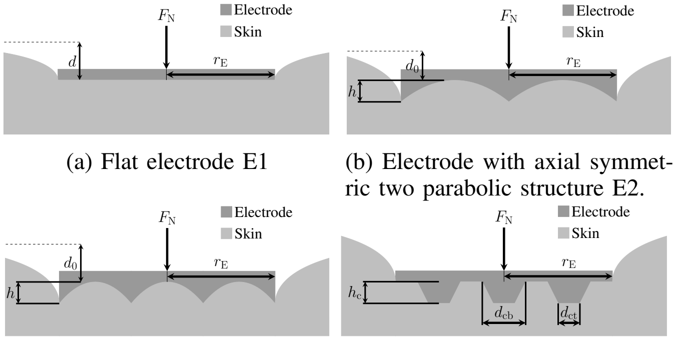

(a) Flat electrode E1

(b) Electrode with axial symmetric two parabolic structure E2.

(c) Electrode with axial symmetric three parabolic structure E3.

(d) Electrode with truncated cone structure E4.

Fig. 2: Electrode cross section.

B. Electrode Geometries

In order to compare the influence of electrode sizes in ranges of typical commercially available electrodes, three flat electrodes E1 with different radii $r_\mathrm{E} = \{8\,\mathrm{mm},\ 10\,\mathrm{mm},\ 12\,\mathrm{mm}\}$ were chosen. In addition, adding a surface structure can increase the effective contact area between the electrode and the skin surface without increasing the electrode radius. Furthermore, a surface structure could have a positive influence on the mechanical stability of the contact and could prevent movement artifacts [6]. Therefore, three electrodes with different surface structures have been examined. In order to create full contact between a structured indenter, such as the electrodes considered here, and the skin, the mechanical stress beneath the indenter must exceed a specific threshold. The mechanical stress can be calculated analytically for axial symmetric indenters using the method of dimensionality reduction for certain profiles [7]. The resulting analytical expression leads to a direct relationship between the geometric properties of the profile and the normal force F_N required for full contact. This expression allows to easily make adjustments regarding the geometric properties and the measurement setup. Therefore, the two axial symmetric concave parabolic structured electrodes E2 and E3 were examined in this research. A nub structure leads to particularly good mechanical adhesion and has already been used in other investigations [6, 8, 9], although the structure itself has not been investigated so far. For this reason an electrode with a nub structure E4 has been investigated. The electrode profiles and their geometric properties are illustrated in Fig. 2. The geometric properties of the two parabolic structured electrode E2 from Fig. 2b, the three parabolic structured electrode E3 from Fig. 2c and the nub structured electrode E4 from Fig. 2d are summarized in TABLE I.

C. Additive Manufacturing of Electrodes

Additive manufacturing, also known as 3D printing, allows a design to be converted into a finished component quickly and cost-efficiently [10, 11]. With regard to the electrodes developed here, the main advantage of this manufacturing process is that the electrodes can be manufactured in a single process step. Furthermore, the structured surface profiles can be created by adding material. Although there are many different additive manufacturing processes, only a few are able to produce electrically conductive structures. One of these methods is fused deposition modeling (FDM), which is used in this study. For this purpose, a geometric 3D model was created in the CAD software SolidWorks by Dassault Systèmes SolidWorks Corp., which was then converted into machine commands by the slicing software Ultimaker Cura by Ultimaker. The printer used is the Creality CR6-SE, which was equipped with an $0.8\,\mathrm{mm}$ nozzle. The electrodes were made entirely of the filament conductive PLA from Proto-Pasta, which gets its conductivity from added carbon black. The parameters used during the slicing and printing process are listed in Table II. These parameters have led to the best printing results. Note that if a parameter is not listed, its default value has been used. A photo of the manufactured electrodes is given in Fig. 3.

TABLE I: Geometric properties of the structured electrodes

Properties	Electrode E2	E3	E4
Radius r_E	$10\,\mathrm{mm}$	$10\,\mathrm{mm}$	$10\,\mathrm{mm}$
Height h	$0.72\,\mathrm{mm}$	$0.72\,\mathrm{mm}$	$0.36\,\mathrm{mm}$
Diameter d_cb	-	-	$1.6\,\mathrm{mm}$
Diameter d_ct	-	-	$1.2\,\mathrm{mm}$
Number of cones N_c	-	-	31

TABLE II: Slicing and printing parameters

Parameter	Value
Nozzle diameter	$0.8\,\mathrm{mm}$
Layer height	$0.12\,\mathrm{mm}$
Wall thickness	$1.6\,\mathrm{mm}$
Top thickness	$0.24\,\mathrm{mm}$
Bottom Thickness	$0.48\,\mathrm{mm}$
Infill density	100%
Infill pattern	Concentric
Printing temperature	$215\,°\mathrm{C}$
Build plate temperature	$60\,°\mathrm{C}$
Infill speed	$30\,\mathrm{mm\,s^{-1}}$
Wall speed	$15\,\mathrm{mm\,s^{-1}}$
Support pattern	Concentric
Support interface pattern	Lines

D. Measurement Setup

In order to characterize the electrical contact behaviors of the electrodes, impedance measurements were carried out. The chosen measurement setup is shown in Fig. 4. Since measurements of single electrode-skin interface impedances are not possible, the total impedance

$$Z = 2Z_\mathrm{E} + Z_\mathrm{T} \tag{1}$$

is determined. One measurement was carried out to determine the dependence on the contact area and another to determine the influence of the surface structure. In this study, series of measurements were recorded on a total of four subjects. This study has been approved by the institutional ethics board of the University of Lübeck (declaration number 21-020). The electrodes are placed to the subject's forearm with the aid of a compression bandage. The electrodes placed in the

(a) Electrodes placed inside compression bandage. (b) Manufactured electrodes with different surface structures.

Fig. 3: Photo of additively manufactured dry electrodes.

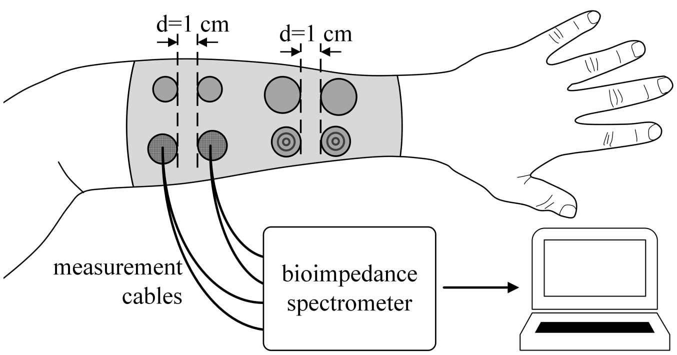

Fig. 4: Measurement setup to determine the electrode-skin interface impedances of different dry electrodes.

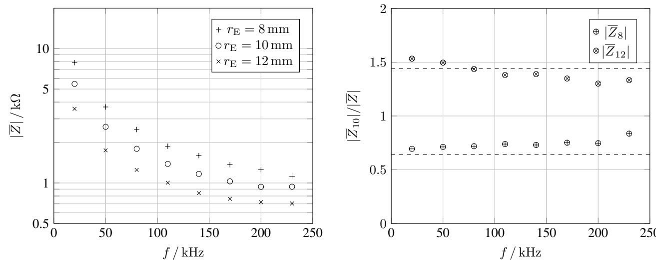

(a) Impedance magnitude. (b) Normalized impedance magnitudes.

Fig. 5: Dependency of the impedance on the contact area.

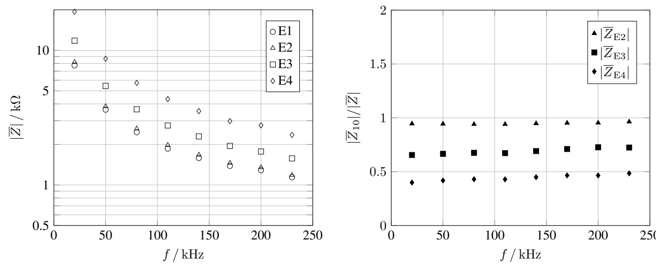

(a) Impedance magnitude (b) Impedance magnitude normalized.

Fig. 6: Dependency of the impedance on the structured electrode surface.

compression bandage are shown in Fig. 3a. The distance between the electrodes is $1\,\mathrm{cm}$. For each measurement, one compression bandage was fitted with the electrodes, one with the flat electrodes of different sizes and one with the structured electrodes together with additional flat electrodes as a comparison pair. One bandage was worn on the left arm and the other on the right arm. Before the measurement, the bandages were already worn for 10 minutes in order to reduce temporal influences on the measurement. The measurement duration is 5 seconds per measurement, with two measurements being carried out for each pair of electrodes. The pairs of electrodes are connected to an impedance spectrometer, which is based on a previously published system [12]. This device records the total impedance magnitude $|Z|$, composed of both the electrode-skin contacts and the bioimpedance in-between, in a frequency range between 20 kHz...230 kHz using the four-wires measurement technique.

III. Results and Discussion

A. Radius Dependency

The magnitude frequency response of the impedance $|\overline{Z}|$ averaged over all subjects for the examined electrode radii is shown in Fig. 5. The impedance magnitude decreases from $7\,\mathrm{k\Omega}$ at $f = 20\,\mathrm{kHz}$ to $3\,\mathrm{k\Omega}$ at $f = 230\,\mathrm{kHz}$ for all electrode radii, which is reasonable due to the capacitive behavior of the structure as well as comparable to literature values [4, 13]. Furthermore, it can be seen that the impedance decreases as the radius increases. This observation is consistent with the previous considerations. This relationship is even clearer from the normalized representation in Fig. 5b. This graphic shows the magnitude frequency response of the electrode with the radius $r_\mathrm{E} = 10\,\mathrm{mm}$ normalized to the other magnitude frequency responses. The dashed lines are the ratios of the electrode areas.

B. Surface Texture Dependency

In the following, the influence of the surface structure of the electrodes on the impedance is to be evaluated. As in section III-A, the magnitude frequency response of the impedance for the surface structures to be examined is shown in Fig. 6a. The figure shows that the electrode without a structure E1 has the lowest impedance value. The electrodes with the nub structure E4, on the other hand, provides the highest impedance magnitude. Fig. 6b shows the magnitude frequency response of the electrode E1 from Fig. 6a normalized to the magnitude frequency responses of the structured electrodes. As in the previous experiment, the conditions are approximately constant over the frequency range under consideration. Contrary to the observations from section III-A, the impedance of the electrode-skin contact is not reduced despite the enlargement of the electrode surface through a surface structure. It can even be stated that the more structured the surface, the higher the impedance of the examined contacts. Since only geometric changes were made to the electrodes here, only these can be assumed to be the reason.

One explanation for this observation could be that there is not full contact between the electrode and the skin surface, so the expected increase in effective contact area does not occur and therefore causes a negative impact on the contact impedance. One possible reason for the incomplete contact can be found in the manufacture of the electrodes. The electrodes are manufactured using the FDM process. A filament, in this case the conductive PLA, is placed in lanes on the print bed through a nozzle. Since each of these lanes has a fixed height, a kind of staircase pattern results when bevels are printed. This can result in mechanical electrode-skin contact that is only at the edges of the pattern. This would significantly reduce the contact area.

On the other hand, the test setup can also have a negative impact on the mechanical contact. When developing the surface structures, it was assumed that the contact causes an indentation, where only the electrode is allowed to experiences a normal force F_{N} in the direction of the skin surface. The corresponding normal force is generated by the compression bandage. This not only affects the electrodes, but also the surrounding skin. The assumption of an ideal indenter is therefore not sufficient, since the electrodes are not deflected in relation to the skin to the extent required for complete contact.

IV. Conclusion and Outlook

The designed and additively manufactured electrodes proposed in this work show a similar behavior like conventional dry electrodes and could therefore be useful in many biosignal acquisition applications. The decrease in impedance magnitude over frequency as well as the strong relationship between electrode radius and the electrode-skin impedance correspond to the simple electrical equivalent circuit. However, a decrease of the interface impedance via specific surface textures could not be achieved. It is assumed that this effect is caused by a combination of the additively manufactured surface characteristics, the specific dimensions of the textures and the inappropriate force application to the electrodes. An approach for improving the surface quality, especially to address the problem of step patterns could be the use of a smaller nozzle diameter. This would have the advantage that a higher resolution would be achieved, especially with small structures such as the nubs. Furthermore, the staircase pattern could be removed by a grinding process. The problem of indentation must be examined more closely in future studies. For this purpose, an attempt should be made, where a force is only applied to the electrodes.

Acknowledgement

This work was supported by European Union – European Regional Development Fund, the Federal Government and Land Schleswig Holstein, Project: "Diagnose- und Therapieverfahren für die Individualisierte Medizintechnik (IMTE)", Project No. 12420002.

References

[1] Yu Mike Chi, Tzyy-Ping Jung, and Gert Cauwenberghs. "Dry-Contact and Noncontact Biopotential Electrodes: Methodological Review". In: *IEEE Reviews in Biomedical Engineering* 3 (2010), pp. 106–119.

[2] Guangli Li, Sizhe Wang, and Yanwen Y. Duan. "Towards gel-free electrodes: A systematic study of electrode-skin impedance". In: *Sensors and Actuators B: Chemical* 241 (2017), pp. 1244–1255.

[3] C. Pylatiuk et al. "Comparison of surface EMG monitoring electrodes for long-term use in rehabilitation device control". In: *2009 IEEE International Conference on Rehabilitation Robotics*. 2009, pp. 300–304.

[4] R Kusche, S Kaufmann, and M Ryschka. "Dry electrodes for bioimpedance measurements—design, characterization and comparison". In: *Biomedical Physics and Engineering Express* 5.1 (Nov. 2018), p. 015001.

[5] Anna Gruetzmann, Stefan Hansen, and Jörg Müller. "Novel dry electrodes for ECG monitoring". In: *Physiological Measurement* 28.11 (Oct. 2007), pp. 1375–1390.

[6] Anas Albulbul. "Evaluating Major Electrode Types for Idle Biological Signal Measurements for Modern Medical Technology". In: *Bioengineering* 3 (Aug. 2016), p. 20.

[7] Valentin L. Popov, Markus Heß, and Emanuel Willert. *Handbook of contact mechanics : exact solutions of axisymmetric contact problems*. Berlin, Heidelberg, Apr. 2019.

[8] Lana Popović-Maneski et al. "Properties of different types of dry electrodes for wearable smart monitoring devices". In: *Biomedical Engineering / Biomedizinische Technik* 65.4 (2020), pp. 405–415.

[9] Bahareh Taji, Adrian D. C. Chan, and Shervin Shirmohammadi. "Effect of Pressure on Skin-Electrode Impedance in Wearable Biomedical Measurement Devices". In: *IEEE Transactions on Instrumentation and Measurement* 67.8 (2018), pp. 1900–1912.

[10] Vlads Vladinovskis. "Review of 3D Printing Technologies and Considerations on Their Use in Orthopedy". In: *2020 IEEE 61th International Scientific Conference on Power and Electrical Engineering of Riga Technical University (RTUCON)*. 2020, pp. 1–6.

[11] Leonardo Rosa Ribeiro da Silva et al. "A comprehensive review on additive manufacturing of medical devices". In: *Progress in Additive Manufacturing* 6 (Aug. 2021).

[12] Roman Kusche and Martin Ryschka. "Combining Bioimpedance and EMG Measurements for Reliable Muscle Contraction Detection". In: *IEEE Sensors Journal* 19.23 (2019), pp. 11687–11696.

[13] Antonio Bosnjak et al. "Characterizing dry electrodes impedance by parametric modeling for arm wearable long-term cardiac rhythm monitoring". In: *2017 Computing in Cardiology (CinC)*. 2017, pp. 1–4.